Published in final edited form as:
Biochim Biophys Acta. 2008 November ; 1778(11): 2544–2554. doi:10.1016/j.bbamem.2008.07.013.

Interactions of the C-terminus of pulmonary surfactant B with lipid bilayers are modulated by acyl chain saturation

Vijay C. Antharam[*], **R. Suzanne Farver**[*], **Anna Kuznetsova**[*], **Katherine H. Sippel**[*], **Frank D. Mills**[*], **Douglas W. Elliott**[*], **Edward Sternin**[1], and **Joanna R. Long**[*]

[*]*Department of Biochemistry and Molecular Biology and McKnight Brain Institute, Box 100245, Gainesville, FL 32610-0245*

[1]*Department of Physics, Brock University, St. Catharines, Ontario Canada, L2S 3A1*

Summary

Lung surfactant protein B (SP-B) is critical to minimizing surface tension in the alveoli. The C-terminus of SP-B, residues 59-80, has much of the surface activity of the full protein and serves as a template for the development of synthetic surfactant replacements. The molecular mechanisms responsible for its ability to restore lung compliance were investigated with circular dichroism, differential scanning calorimetry, and ^{31}P and ^{2}H solid-state NMR spectroscopy. SP-B_{59-80} forms an amphipathic helix which alters lipid organization and acyl chain dynamics in fluid lamellar phase 4:1 DPPC:POPG and 3:1 POPC:POPG MLVs. At higher levels of SP-B_{59-80} in the POPC:POPG lipid system a transition to a nonlamellar phase is observed while DPPC:POPG mixtures remain in a lamellar phase. Deuterium NMR shows an increase in acyl chain order in DPPC:POPG MLVs on addition of SP-B_{59-80}; in POPC:POPG MLVs, acyl chain order parameters decrease. Our results indicate SP-B_{59-80} penetrates deeply into DPPC:POPG bilayers and binds more peripherally to POPC:POPG bilayers. Similar behavior has been observed for KL_4, a peptide mimetic of SP-B which was originally designed using SP-B_{59-80} as a template and has been clinically demonstrated to be successful in treating respiratory distress syndrome. The ability of these helical peptides to differentially partition into lipid lamellae containing varying levels of monounsaturation and subsequent changes in lipid dynamics suggest a mechanism for lipid organization and trafficking within the dynamic lung environment.

Keywords

lung surfactant; surfactant protein B; respiratory distress syndrome; lipid bilayers; ^{31}P NMR; ^{2}H NMR

Introduction

A fundamental problem associated with breathing stems from the high surface area of the lung: the need to minimize surface tension in small, gas-containing, aqueous lined structures. The task of reducing surface tension and increasing lung compliance is accomplished by lung

Address correspondence to: Dr. Joanna R. Long, Box 100245, Department of Biochemistry and Molecular Biology, University of Florida, Gainesville, FL 32610-0245 Telephone: 352-846-1506, Fax: 352-392-3422. Corresponding author's email: E-mail: jrlong@mbi.ufl.edu.

surfactant. Lung surfactant protein B (SP-B), which directly interacts with the phospholipids in surfactant, is particularly critical to its function [1]. Mature SP-B is a homodimer, made up of two 79-81 amino acid monomers, that is extremely hydrophobic, containing high levels of valine, leucine, isoleucine, alanine, phenylalanine, and tryptophan [2-4]. SP-B has a net cationic charge > +5 at physiologic pH. The native form of the protein contains 6 cysteines that form intramolecular disulfide bonds and a seventh cysteine residue that forms an intermolecular disulfide bond. The conservation of the 6 cysteines that form intramolecular disulfide bridges, the pattern of disulfide formation, and its hydrophobicity place SP-B in the saposin family of proteins. Other proteins in the saposin family include amoebapores from *Entamoeba histolytica*, acid sphingo-myelinase, acyloxyacyl hydrolase, and sphingolipid activator proteins A-D (saposins A-D) [5]. The higher hydrophobicity of SP-B and cysteine 48 which forms the disulfide bridge connecting monomers make SP-B unique among the members of the saposin family. The hydrophobicity and disulfide bridges in SP-B also make purification or heterologous expression of the protein in large quantities impractical. Synthetic, peptide-based lung surfactant replacements for treatment of RDS have received notable attention as they remove the immunologic risks associated with animal-derived surfactants [6-8].

While the entire 80 amino acid SP-B protein is essential for lung surfactant organization, dynamics and respiration, fragments of the native sequence have shown significant biophysical function, particularly peptides corresponding to the N-terminal and C-terminal 20-25 amino acids [3,9]. To date, the N-terminal region of the peptide, specifically residues 1-25, has been more extensively studied in terms of its molecular properties and possible structural adaptation in different lipid environments. While both peptides have considerable surface activity, activity similar to native SP-B has only been achieved with a chimeric construct of the two peptides [10]. Both peptides form cationic amphipathic helices in SDS micelles and SP-B_{1-25} has been determined to be helical in lipid environments[11-14], but their individual roles in lipid trafficking are not well understood. The preponderance of leucines and relative lack of prolines and aromatic sidechains in the C-terminus distinguish it from the N-terminus, which contains four prolines as well as a phenylalanine and a tryptophan. The peptides also have varying spacing between hydrophilic and hydrophobic amino acids. These differences could lead to varying secondary structures and penetration into lipid lamellae as well as different effects on phospholipids dynamics.

The C-terminal fragment of SP-B, specifically residues 59-80, (SP-B_{59-80}) has shown efficacy in altering phospholipid properties based on *in vitro* assays measuring surface tension, such as pulsating bubble surfactometry, as well as *in vivo* assays demonstrating gain of function in surfactant-deficient fetal rabbits [3]. As with the N-terminus, the C-terminal peptide is believed to form an amphipathic helix involved in lipid organization, but direct structural measurements in varying lipid contexts have to date not been documented. A recent solution NMR study of the C-terminus of SP-B (residues 63-78) reconstituted in either SDS micelles or the organic solvent HFIP found the first five residues to be unstructured and established that the rest of the sequence formed a helix in both SDS micelles and organic solvent [13]. A previous CD study [12] of SP-B_{59-80} in TFE and SDS micelles and the solution NMR study are the only documented structural assessments of the C-terminal region of SP-B. While these measurements predict the last 21 amino acids of SP-B to be helical, it should be noted that its exact structural adaptation in a lipid environment, where its function in lipid adsorption and resorption is most important, may vary. Also, a canonical α-helical conformation (3.6 residues/turn) leads to unfavorable placement of the charged residues in a lipid milieu. Despite the scarcity of literature pertaining to residues 59-80 of SP-B, it is widely believed that many *in vivo* activities of SP-B are fulfilled by the C-terminal end based on both *in vitro* and *in vivo* studies [3,10]

Of particular clinical interest, the last 22 amino acids of SP-B served as the template for designing the KL_4 peptide, KLLLLKLLLLKLLLLKLLLLK [8]. The basis of the sequence for KL_4 was the charge distribution and hydrophilic/hydrophobic ratio of the primary sequence of SP-B_{59-80}. To date, KL_4 has enjoyed the most clinical success as a potential synthetic replacement for SP-B [15-19]. While KL_4 was developed based on the hydrophilic/hydrophobic pattern in SP-B_{59-80}, their primary sequences have only modest similarity with SP-B_{59-80} containing negatively charged terminal amino acids and variable spacing of three-four hydrophobic residues between polar or charged residues. A significant question remaining is whether KL_4 and SP-B_{59-80} act similarly, despite clear deviations at the primary amino acid level. Based on its charged distribution and CD and FTIR studies of intact SP-B in lipid environments, SP-B is thought be comprised of amphipathic helices at lipid interfaces [20, 21]. However, an FTIR study of KL_4 in DPPC/DPPG concluded the peptide formed a helix spanning the bilayers and it has been posited that KL_4 might more closely mimic lung surfactant protein C (SP-C) rather than the C-terminus of SP-B [22]. More recent IR and NMR studies of KL_4 conclude that it binds to the lipid interface but its structure and penetration are lipid and pressure dependent[23-25]. One key to understanding how similar KL_4 is to SP-B_{59-80} in its behavior is to examine the binding of SP-B_{59-80} to model lipid membrane systems, its effects on their dynamics, and any effects on the L_β to L_α phase transition in DPPC lipids; these results can then be directly compared to previous studies of KL_4. Thus, we chose to study the effects of SP-B_{59-80} on 4:1 DPPC:POPG and 3:1 POPC:POPG MLVs. The former composition is similar to formulations commonly used in studying lung surfactant, while the latter is a paradigm lipid system commonly employed to probe peptide/lipid interactions, particularly in studies of cationic, amphipathic helices [26-28]. Lipid phases of these compositions could also be found in localized areas of the alveoli during the breathing cycle [29].

Based on understanding the properties of SP-B_{59-80}, new non-natural peptide analogs of SP-B that exploit the protein's qualities in altering lipid dynamics could be made to extend or enhance artificial lung surfactant therapies. Thus, understanding how SP-B_{59-80} affects the molecular and biophysical properties of the lipids is of particular relevance to the treatment of various forms of RDS.

Materials and Methods

Synthesis of SP-B_{59-80}

SP-B_{59-80}, (DTLLGRMLPQLVCRLVLRCSMD) was synthesized via solid-phase peptide synthesis on a Wang resin (ABI 430, ICBR, UF) and cleaved from the resin with King's reagent and ether precipitated. The cleaved product was purified via RP-HPLC using a C18 Vydac column with a water/acetonitrile gradient (containing 0.3% TFA). The fractions corresponding to SP-B_{59-80} were collected and purity of the product was verified by mass spectrometry with a mass to charge ratio of (m/z) of 2533. Dried peptide was weighed and dissolved in methanol to a stock concentration of approximately 1 mM, and aliquots were analyzed by amino acid analysis for a more accurate determination of concentration (Molecular Structure Facility, UC Davis).

Heterologous expression of a SP-B_{59-80} double mutant (SP-B'_{59-80})

For later experiments, SP-B'_{59-80} was expressed using a pET31 construct (EMD Biosciences, Inc., Gibbstown, NJ) incorporating a codon-optimized synthetic gene for SP-B_{59-80} (DNA2.0, Menlo Park, CA) in *BL21(DE3)* cells with subsequent purification and cleavage using established protocols [30]. The expressed sequence of SP-B'_{59-80} was modified to incorporate isoleucines in lieu of methionines (DTLLGRILPQLVCRLVLRCSID) for compatibility with a cyanogen bromide cleavage reaction. Following HPLC purification of the final product, fractions corresponding to SP-B'_{59-80} were collected and their purity was verified by mass

spectrometry with a mass to charge ratio of (m/z) of 2497. Dried peptide was weighed and dissolved in methanol to a stock concentration of approximately 1 mM, and aliquots were analyzed by amino acid analysis for a more accurate determination of concentration (Molecular Structure Facility, UC Davis). This peptide was used to obtain results shown in Figures 1, 5, 6, and 11 as well as the POPG-d_{31} results in Figures 9 and 10. Its effects on lipid dynamics were ascertained to be identical to those of the native sequence.

Preparation of Peptide:Lipid Samples

POPC, DPPC, POPG, POPC-d_{31}, DPPC-d_{62} and POPG-d_{31} were purchased as chloroform solutions (Avanti Polar Lipids, Alabaster, AL) and concentrations were verified by phosphate analysis [31] (Bioassay Systems, Hayward, CA). The lipids were mixed at a molar ratio of 4:1 DPPC:POPG and 3:1 POPC:POPG in chloroform and aliquoted. For samples containing peptide, a methanol solution of SP-$B_{59\text{-}80}$ was added to lipid solutions with final protein: lipid (P:L) molar ratios ranging from <1:1000 to >1:50. The samples were dried under a stream of nitrogen with the sample temperature maintained at 42-50° in a water bath; the resulting films were suspended in cyclohexane, flash-frozen, and lyophilized overnight to remove residual solvent.

CD experiments

3 mg of peptide-lipid powder was solubilized in 1 mL of 10 mM HEPES buffer at pH 7.4, with 140 mM NaCl, to achieve a concentration of 40 μM SP-$B_{59\text{-}80}$ with 4 mM lipids. Samples were placed in a 50 °C water bath to facilitate solubilization accompanied by 3-5 freeze thaw cycles with vortexing to achieve equilibration. Peptide-lipid MLVs were extruded through 100nm filters (Avanti Polar Lipids, Alabaster, AL) 15-25 times above the T_m of the lipids to form LUVs just prior to CD analysis. CD experiments were performed on an Aviv Model 215 (Lakewood, NJ) at 45 °C using a 195-260 nm wavelength range, a 1 nm step size and averaging of 40-50 scans. Background contributions from the buffer and LUVs were removed by subtracting appropriate controls.

DSC analysis

For each DSC sample, 2.2 mg of peptide-lipid powder was solubilized in 1 mL 5 mM HEPES buffer at pH 7.4, with 140 mM NaCl and 1 mM EDTA to achieve a 3 mM lipid concentration. Samples were placed in a 50 °C water bath to facilitate solubilization accompanied by 3-5 freeze thaw cycles with vortexing to achieve equilibration. Peptide-lipid MLVs were extruded through 100 nm filters (Avanti Polar Lipids, Alabaster, AL) 15-25 times at 45 °C to form LUVs and degassed just prior to DSC. DSC experiments (Microcal Inc, LLC Northampton) were conducted over a range of 10-70 °C at a scan rate of 1 °C/min and run in triplicate.

Solid state NMR analysis

For each solid-state NMR sample, 30 mg of peptide-lipid powder was placed in a 5 mm diameter NMR tube and 200 μL of buffer containing 5mM HEPES at pH 7.4, 140mM NaCl, and 1mM EDTA in ^2H depleted water (Cambridge Isotopes, Andover MA) was added. Samples were made using 4:1 DPPC-d_{62}:POPG, 4:1 DPPC:POPG-d_{31}, 3:1 POPC-d_{31}:POPG, and 3:1 POPC:POPG-d_{31} lipid preparations. NMR samples were then subjected to 3-5 freeze-thaw cycles with gentle vortexing to form MLVs. ^{31}P and ^2H NMR data were collected on 500 and 600 MHz Bruker Avance systems (Billerica, MA) using a standard 5 mm BBO probe. For the ^{31}P NMR experiments, 25 kHz proton decoupling was employed during acquisition to remove dipolar couplings. Spectra were acquired at 34, 39, and 44 °C to verify sample equilibration with 1024-2048 scans and a 5 second recycle delay between scans to minimize RF sample heating. For the ^2H NMR experiments, data were collected using a quad echo sequence (90°-τ-90°-τ-acq with $\tau = 30$ μs) with a B_1 field of 40 kHz. Spectra were acquired at

34, 39, and 44 °C with 1024 or 2048 scans and a 0.5 second recycle delay between scans. To monitor the phase transitions of the lipids, for some samples spectra were also collected over a range of 30-44 °C in 2° increments.

DePaking of NMR data was accomplished with previously published algorithms which simultaneously dePake and determine macroscopic ordering in partially aligned lipid spectra using Tikhonov regularization [32]. ^{31}P NMR spectra were referenced to phosphate buffer prior to dePaking and dePaked spectra were quantitated by fitting the two peaks with Lorentzian line shapes. Assignments of ^{2}H resonances were made based on published values for DPPC [33,34].

Results

Secondary structure

The CD spectra at 45 °C of SP-B′$_{59-80}$ incorporated into lipid vesicles are shown in Figure 1. The CD spectra are characterized by double minima at 206-208 and 222 nm, as is typically seen for peptide helices. Interestingly, the spectra have a minimum ellipticity at 206-208 significantly lower than the minimum at 222 nm. Similar spectra have been observed for KL_4 in DPPC:POPG LUVs [24] and peptides which are constrained to form π-helices in buffer [35]. Interpretation of the CD spectra in terms of helix content is complicated by the fact that SP-B$_{59-80}$ does not form a typical amphipathic α-helix when projected on a helical wheel. Fitting of the CD data with standard deconvolution software [36] led to secondary structure estimates of 75-82% α-helix, 17-23% random coil, and negligible β-sheet for SP-B$_{59-80}$ interacting with POPC:POPG LUVs. Secondary structure estimates of 98-100% α-helix with negligible random coil and β-sheet populations were seen for SP-B$_{59-80}$ interacting with DPPC:POPG LUVs. However, the quality of the fits was poor due to the non-standard shape of the CD spectra and poor quality of the data below 200 nm due to light scattering from the lipids.

DSC indicates SP-B$_{59-80}$ has little effect on DPPC:POPG lipid miscibility

Figure 2 shows DSC thermograms for 4:1 DPPC-d$_{62}$:POPG LUVs containing varying levels of SP-B$_{59-80}$. The phase transition is not dramatically influenced by the presence of SP-B$_{59-80}$, although it moves to slightly higher temperatures with increasing peptide concentration. In contrast, KL_4 has been shown by DSC and fluorescence microscopy to promote lipid phase separation and domain formation [24,37,38]; no effects on the lipid miscibility are seen at any molar percentages of SP-B$_{59-80}$ studied here. The peak-width at half height, or $\Delta T_{1/2}$, does not change significantly upon addition of SP-B$_{59-80}$ indicating that the cooperativity of the phase transition is not markedly influenced by the addition of SP-B$_{59-80}$. The relative differences between KL_4 and SP-B$_{59-80}$ are not completely unexpected as KL_4 contains solely hydrophilic residues that are cationic while SP-B$_{59-80}$ contains a mixture of cationic and anionic residues. Thus, partitioning of KL_4 with POPG may be more energetically favorable, enhancing phase separation in DPPC/POPG mixtures below the phase transition temperature of DPPC.

The interaction of SP-B$_{59-80}$ with lipid headgroups

^{31}P solid-state NMR for 4:1 DPPC:POPG and 3:1 POPC:POPG MLVs with varying levels of SP-B$_{59-80}$ were collected to assess the effect of this peptide on lipid phases and the orientation of the phospholipid headgroups. Shown in Figure 3 are ^{31}P spectra for the DPPC-d$_{62}$:POPG samples at 44° C. Also shown are the dePaked spectra allowing a clear determination of the individual, time-averaged CSAs of the PC and PG headgroups. Only lamellar phases are observed and the resonance for the POPG lipids moves with addition of peptide; this is more evident after dePaking the spectra. As seen in other studies [24,39,40], spontaneous macroscopic lipid alignment occurs in the magnetic field. Due to this phenomenon, normally

spherical MLVs undergo a deformation to more ellipsoidal geometries, distorting the powder spectra. The extent of magnetic field alignment was accounted for in the dePaking algorithm [32]. The difference in PG and PC CSAs is due to the difference in their preferred headgroup orientations relative to the membrane normal [41]. With increasing levels of SP-B_{59-80}, the PC CSA is invariant, but the PG CSA lessens with increasing peptide levels. The CSA for POPG alone is significantly smaller than observed for POPG in 4:1 DPPC:POPG or 3:1 POPC:POPG mixtures prior to the addition of SP-B_{59-80} [24]. However, for the binary 4:1 DPPC:POPG mixture containing higher concentrations of SP-B_{59-80}, the ^{31}P CSAs are more comparable to those of the neat lipids. Thus, SP-B_{59-80} is clearly affecting the interactions of the PC and PG lipids.

Shown in Figure 4 are ^{31}P spectra for the POPC-d_{31}:POPG samples at 44° C and their dePaked counterparts. For 3:1 POPC:POPG MLVs, addition SP-B_{59-80} leads to a considerably smaller decrease in the PG CSA; in contrast, KL_4 which has similar effects on the PG CSA in both DPPC:POPG and POPC:POPG mixtures. Based on these results, when POPG is interacting with PC headgroups, electrostatic interactions cause the PG headgroups to reorient leading to a subsequent increase in their averaged CSA values. Addition of surfactant peptide disrupts this interaction, causing the PG CSAs to move toward values seen for POPG alone; if the surfactant peptide is highly cationic, electrostatic interactions lead to similar decreases in the POPG CSA regardless of whether the PC lipid is fully saturated or monounsaturated [24]. In the case of SP-B_{59-80}, the negatively charged amino acids at the termini result in less electrostatic interaction between the peptide and the PG headgroup. However the partitioning of the peptide into the DPPC:POPG lipids is sufficient to significantly alter the orientation of the PG headgroup due to its overall effects on lipid packing and dynamics; in POPC:POPG lipids it is not. The ^{31}P NMR spectra for 3:1 POPC-d_{31}:POPG MLVs containing varying concentrations of SP-B_{59-80} are typical for lamellar phases up to 1.7 mol% peptide (Figure 4). However, the spectrum at 2.5 mol% peptide suggests the onset of other bulk dynamics in the lipids, consistent with exchange between a lamellar phase and either a micellar phase or a hexagonal phase. With the onset of a phase transition at 2.5 mol% peptide, no clear distinction between the PC and PG lipids can be made.

^{2}H NMR studies of DPPC:POPG lipid miscibility on addition of SP-B_{59-80}

To determine whether addition of SP-B_{59-80} causes phase separation of the DPPC and POPG lipids, ^{2}H NMR spectra were collected over the temperature range of the phase transitions for samples which contained either deuterated DPPC or deuterated POPG (Figure 5). A second moment analysis of the data was used to determine the phase transition temperatures of the individual lipids (Figure 6). From these spectra, it is clear that in the 4:1 DPPC:POPG samples the lipids are fully miscible with the DPPC and POPG melting at similar temperatures. The phase transition seen for deuterated DPPC is at a slightly *lower* temperature (midpoint of 30.6 °C) than for deuterated POPG (32.7 °C). This is in part due to the fact that a larger percentage of the fatty acyl chains are deuterated (80% vs. 10%) [42] but may also reflect slight differences in POPG content between the two samples since they were made from different lipid stock solutions. For the samples that do not contain SP-B_{59-80}, the spectra at intermediate melting temperatures are a superposition of gel phase and liquid phase spectra. Addition of SP-B_{59-80} affects the phase transition temperature of both lipids with the phase transition temperature for DPPC-d_{62} increasing to 31.5 °C and the POPG-d_{31} phase transition temperature decreasing to 30.3 °C. On addition of SP-B_{59-80}, at lower temperatures the POPG-d_{31} spectra have a larger percentage of the dynamic lipid phase evident and in the DPPC-d_{62} spectra the dynamic phase is absent, as can be seen by comparing spectra at 30 °C and 32 °C. The peptide also leads to an increase in temperature at which the lipids are completely melted (34 °C vs. 38 °C for deuterated DPPC; 36 °C vs. 38 °C for deuterated POPG), consistent with the DSC data. Attempts to determine the fractions of liquid phase and gel phase by spectral

subtractions with samples containing differing percentages of SP-B_{59-80} were unsuccessful due to variations in the lipid alignment and acyl chain order parameters. Thus, addition of SP-B_{59-80} leads to some phase separation of the lipids at lower temperatures with a significant fraction of POPG remaining in the gel phase; at higher temperatures, the lipids exhibit similar spectra consistent with the lipids becoming fully miscible. These differences are too subtle to be observed via differential scanning calorimetry. Above the phase transition temperature of the domain with the higher T_m, the peaks in the ^2H spectra coalesce to a single resonance for each position in the acyl chains suggesting the absence of separate domains in the fluid phase or exchange between domains is fast on the NMR time scale.

Effects of SP-B_{59-80} on lipid acyl chains

^2H NMR spectra of DPPC-d_{62}:POPG and POPC-d_{31}:POPG MLVs at 44 °C with varying levels of SP-B_{59-80} (Figures 7 and 8) allow determination of the effect of this membrane-active peptide on lipid dynamics in the fluid phase and insight into the depth of peptide penetration. For 3:1 POPC-d_{31}:POPG MLVs, decreases are seen in the ordering of the POPC *sn*-1 acyl chains on addition of SP-B_{59-80}. This suggests the peptide binds to the interface, increasing the lateral spacing between the lipids, allowing more motion in the acyl chains. In contrast, addition of SP-B_{59-80} to 4:1 DPPC-d_{62}:POPG MLVs increases the ordering of the DPPC acyl chains, particularly toward the middle of the bilayer. This suggests either 1) insertion of SP-B_{59-80} deeply into the DPPC:POPG bilayers, restricting the motional freedom of the acyl chains, or 2) an electrostatic interaction of the peptide with the lipid headgroups resulting in a change in the lipid packing and headgroup conformation. Also shown in Figures 7 and 8 are the dePaked spectra which allow assignment of each C-D bond in the acyl chain and determination of the time-averaged order parameters, $\langle S_{CD} \rangle$. For samples in which the lipid bilayers show a tendency to align in the magnetic field, the dePaking must take into account the effects of lipid alignment on the probability distribution function. Assuming the magnetic field leads to an ellipsoidal deformation of the MLVs, the probability distribution becomes [32]:

$$p_{(E)}(\theta) \propto \sin(\theta)[\,1-(1-\kappa_E)\cos^2\theta]^{-2} \tag{1}$$

where κ_E refers to square of the ratio of the long to short axes of the ellipsoids. Using Tikhonov regularization, κ_E and the dePaked spectra were determined simultaneously. Lipid acyl chain order parameter profiles[43] were generated (Figures 9 and 10) by assigning the dePaked spectra, measuring the quadrupolar splitting ($\Delta\nu_Q$) for deuterium atoms at various positions along the acyl chain, and determining their order parameter using equation 2, where $\frac{3}{4}\frac{e^2qQ}{h}$ is the quadrupolar coupling of the deuterium nucleus to the electric field gradient. A static quadrupolar coupling of 167 kHz [44] was assumed in calculating the order parameters.

$$\Delta\upsilon_{Q'} = \frac{3}{4}\frac{e^2qQ}{h}(3\cos^2\theta - 1)S_{CD} \tag{2}$$

Comparison of these order parameter profiles to those for the individual lipids show that the DPPC order parameters for 4:1 DPPC:POPG MLVs with P:L ratios >1:200 are higher than would be expected for DPPC alone [24]. Within the resolution of the ^2H NMR experiment, no phase separation is seen. The profiles also yield a more detailed picture of how SP-B_{59-80} affects the lipid dynamics with carbon positions 9-16 the most affected in the PC lipid acyl

chains for both lipid systems. The effects of SP-B_{59-80} on the PG lipids were similarly monitored by collecting ^{2}H NMR spectra for 4:1 DPPC:POPG-d_{31} and 3:1 POPC:POPG-d_{31} MLVs, dePaking the spectra, and generating order parameter profiles. The order parameter profiles for the *sn*-1 chain on POPG in these lipid mixtures are also given in Figures 9 and 10. In these experiments an overall decrease in ordering of the POPG acyl chains is seen on addition of SP-B_{59-80}. Decreases in the order parameters are seen at all the acyl positions in POPG in 3:1 POPC:POPG MLVs and are slightly larger than the changes for POPC. The POPG acyl chain order parameters in 4:1 DPPC:POPG MLVs do not appear to be as affected by SP-B_{59-80}, however a comparison of the results further down the acyl chain for POPG-d_{31} when mixed with DPPC vs. POPC again demonstrates that the peptide interacts with these lipid systems in a manner dependant on the degree of saturation of the fatty acid chains.

Since SP-B_{59-80} is most likely interacting with both lipid populations in the fluid phase rather than segregating the lipids and interacting with a single phase above the L_{β} to L_{α} phase transition, the changes in POPG-d_{31} and DPPC-d_{62} order parameter profiles on addition of SP-B_{59-80} to DPPC/POPG MLVs may seem to be contradictory. The observed changes in order parameters can be reconciled when the data are viewed as the change in order parameter at each position along the acyl chain on addition of peptide relative to the order parameters of the lipids without the peptide. Shown in Figure 11 are the changes in order parameters at particular methylene positions in the *sn-1* palmitoyl acyl chains for the individual lipids in 3:1 POPC:POPG and 4:1 DPPC:POPG MLVs, respectively, on addition of peptide at a P:L molar ratio on the order of 1:100. From these graphs, the behavior of the PG lipids relative to the PC lipids is clearly offset, but the trends with respect to acyl chain position are similar. The offset of the profiles for the PG lipids is consistent with ^{31}P NMR findings described above showing that association of SP-B_{59-80} with the lipids leads to a change in the orientation PG headgroup and an overall decrease in the ^{31}P CSA for the POPG lipids. Thus, the offset in the PG profiles in Figure 11 relative to the PC profiles does not reflect significantly less internal order in the PG lipid methylene chains per se, but instead reflects a change in the average orientation of the PG lipid director relative to the membrane normal. The degree of offset for the POPG profiles in the DPPC:POPG and POPC:POPG mixtures correlate with the degree to which the POPG ^{31}P CSA is affected by addition of peptide. Thus the addition of SP-B_{59-80} is most likely equally affecting the internal dynamics of the methylene chains in both lipids in a similar manner. From their profiles, the methlyenes in the plateau region are less affected than those further down the acyl chain in the POPC:POPG lipid system. This behavior is similar to changes observed on addition of antimicrobial peptides, which typically cause larger changes in order further down the methylene chain [27, 45, 46], but is in contrast to the interaction of KL_4 [24] or saposin C [47, 48] with monounsaturated lipids, which have a larger effect on the plateau region.

Of particular interest to the roles of SP-B_{59-80} and KL_4 in lung surfactant formulations are their similar effects on 4:1 DPPC:POPG MLVs. Previously we have observed that KL_4*increases* order along the DPPC acyl chains with its greatest effect at the center of the bilayers, and this same trend is seen with SP-B_{59-80}. The profile for POPG shows little change in order toward the center of the bilayers and a decrease in the plateau region. However, as discussed above, these differences reflect a change in the average orientation of the POPG headgroup and if this change in orientation is taken into account, the internal order at individual methylene positions in the POPG acyl chain is likely increasing over the entire length of the acyl chain. Increases in lipid acyl chain ordering have been observed in response to polyelectrolyte binding to lipid headgroups [49,50] as well as in response to the addition of small molecules, such as cholesterol [51,52], or transmembrane peptide helices which partition into the acyl chain region of the lipids [53,54]. In the case of polyelectrolyte binding, larger changes are seen for the plateau region of the lipids reflecting a change in overall orientation of the lipids due to changes in packing of the headgroups. Smaller changes are also seen near the center of the bilayers and

are interpreted as resulting from closer packing of the lipids on binding of the electrolyte. For transmembrane helices similar in length to SP-B_{59-80}, increases in order parameters which are similar in magnitude are seen for both the methylene positions in the plateau region and toward the center of the bilayers; these trends are observed in both POPC and DPPC bilayers. This is expected since insertion of a transmembrane peptide of this length primarily affects the thickness of the bilayer and would interact with both the lipid acyl chains and headgroups across the entire span of the bilayers. In contrast, on addition of cholesterol, larger changes in order parameters are observed toward the center of the bilayer [51] since cholesterol partitions to the bilayer interior and does not strongly interact with the lipid head groups. Interestingly, the effects of SP-B_{59-80} and KL_4 on order in DPPC:POPG bilayers are most similar to cholesterol, suggesting the bulk of each peptide is partitioning deep within the lipid bilayers. The higher degree of ordering toward the center of the bilayer suggests the surfactant peptides are penetrating deeply into the bilayer and decreasing the mobility of the acyl chains. However, the smaller changes seen in the plateau region (carbons 3-8) suggest the peptides do not adopt a transmembrane orientation. The thermodynamic penalty imposed by placing SP-B_{59-80} in a transmembrane orientation would be prohibitive since it would place the hydrophilic amino acids at positions 6, 10, 14, and 16 into the hydrophobic core [55]. Thus, the changes in order parameters indicate SP-B_{59-80} lodges into the hydrophobic region of the bilayer, while maintaining a perpendicular orientation to the bilayer normal. This type of interaction would lead to a negative curvature strain within the lipid bilayers, a phenomenon which has been hypothesized as being important to lung surfactant function [56]. A recent solution NMR study of SP-B_{63-78} bound to SDS micelles found the peptide forms an amphipathic helix at the water interface with the hydrophilic residues solvent accessible [13], consistent with our interpretation.

Looking at the same *sn*-1 C-D positions for POPC-d_{31} in 3:1 POPC:POPG MLVs (Figures 10 and 11), it can be seen that SP-B_{59-80} decreases order by as much as 20%, with the largest decrease in ordering seen for position 15. This strongly correlates to SP-B_{59-80} partitioning at the interface of 3:1 POPC:POPG MLVs and increasing the area per lipid molecule leading to more motion in the acyl chains. A striking decrease in the plateau region is seen at 2.5 mol% peptide along with the appearance of an isotropic peak in the ^2H spectrum (Figure 8), consistent with the ^{31}P NMR data suggesting that this concentration of peptide leads to destabilization of the lamellar phase and exchange of the lipids between a lamellar and nonlamellar phase.

From these results we conclude that the penetration and interaction of SP-B_{59-80} with the lipids in lung surfactant is dependent on the degree of saturation in the lipids. Intriguingly, the peptide penetrates deeply into mixtures containing a high level of saturated lipids even though the order of the fatty acyl chains in these lipids is higher than those in monounsaturated lipids. When interacting with monounsaturated lipids, SP-B_{59-80} binds at the interface and has effects similar to other amphipathic peptides, including antimicrobial peptides, which increase curvature strain in the lipids and can cause micelle formation at higher concentrations. The interaction of SP-B_{59-80} with these binary lipid systems is on the whole very similar to behavior previously seen for KL_4, suggesting the two peptides have very similar mechanisms of binding and similar effects on the dynamics of the lipids.

Discussion

The effects of the C-terminal region of SP-B, specifically residues 59-80, on lipid dynamics and acyl chain ordering were explored in two binary lipid systems that differ in their degree of monounsaturation. SP-B_{59-80} has been used as a template for the design of simple molecules for the treatment of respiratory distress syndrome (RDS), the most notable of these being the 21 amino acid peptide KL_4 which has shown exceptional efficacy in lung surfactant formulations, particularly when compared to more conventional therapies that rely upon

exogenous sources of SP-B [57]. The SP-B_{59-80} peptide is presumed to be helical when interacting with lipids based on the distribution of charged and uncharged residues in its primary amino acid sequence and this is borne out by our CD data. To date, few studies examining the structure of SP-B_{59-80} and its interactions with lipids have been carried out despite its demonstrated surface activity and role in the rational design of KL_4. Additionally, subsequent studies of KL_4 have suggested its properties might be more similar to SP-C, which is a small, highly hydrophobic transmembrane protein in contrast to SP-B, which is found at membrane interfaces. Previously we have examined the structure of KL_4 [25] and found it to be consistent with the peptide partitioning in bilayers with the helix axis perpendicular to the membrane normal, but its depth of penetration is dependent on the degree of saturation in the lipids [24]. Whether SP-B_{59-80} binds similarly to lipid interfaces and affects the properties of the lipids in the same manner is the subject of this study.

While the sequence of KL_4 is based on SP-B_{59-80}, there are some notable differences in their primary amino acid sequences. First, KL_4 contains only two types of amino acids, the hydrophobic leucine and cationic lysine; in SP-B_{59-80} the distribution of hydrophobic and hydrophilic residues is similar, but the hydrophilic amino acids are a mixture of anionic (D_{59} and D_{80}), polar (Q_{68}) and cationic (R_{64}, R_{72}, and R_{76}) residues at physiologic pH. The spacing of lysines in KL_4 is based on the five charged amino acids in SP-B_{59-80}, but the preponderance of long, cationic sidechains would allow more favorable electrostatic interactions with the anionic POPG lipids and phospholipid interfaces in general. If both peptides form amphipathic helices at lipid interfaces, their secondary structure might also differ since the spacing of the polar residues in SP-B_{59-80} is primarily every four residues rather than every five residues, as in KL_4. Finally, we have shown that KL_4 has the ability to deeply embed in DPPC-rich bilayers, which we have attributed to the lysine sidechains being able to snorkel up to the phosphates at the lipid interface [24]. While arginine residues would also allow this behavior, the aspartic acid residue sidechains at the ends of SP-B_{59-80} would be too short and the electrostatic interactions with the phosphate moieties would be unfavorable. Finally the occurrence of a proline residue at position 67 in SP-B_{59-80} could affect the helical nature of the peptide. Nonetheless, both peptides have been demonstrated to be surface active and effective in lowering surface tension at air/water interfaces.

Based on the DSC data, SP-B_{59-80} does not have the same effect on the macroscopic phase properties of DPPC:POPG mixtures as KL_4. DSC experiments performed by Saenz, *et al.* [37] and our group [24] as well as epifluorescence studies [38] indicate that KL_4 mediates phase separation in DPPC:POPG environments. In contrast, DSC indicates SP-B_{59-80} has little effect on the thermodynamic properties of DPPC:POPG LUVs other than small effects on the cooperativity of the L_β to L_α phase transition. However, the ^2H NMR data show there is a small degree of phase separation in the gel phase on addition of SP-B_{59-80}.

In contrast to the calorimetry data, which reports on bulk thermodynamic properties of the lipids, ^{31}P and ^2H NMR data monitoring lipid dynamics above the phase transition temperature show the two peptides interact similarly with lipid vesicles and have similar effects on lipid dynamics in 4:1 DPPC-d_{62}:POPG lipid environments. The ^{31}P NMR data indicate that neither peptide affects the DPPC CSA, while both peptides affect the POPG CSA. While an interaction of SP-B_{59-80} with the anionic PG headgroups is one plausible explanation of this data, it should be noted that SP-B_{59-80} does not possess the distinct cationic charge periodicity found in KL_4; the sole use of lysines for charged residues in KL_4 could allow for a more enhanced electrostatic interaction with PG compared to SP-B_{59-80}. This fact is borne out by quantitative comparison of the data for the two peptides. The changes in the POPG CSA, which report on changes in the average orientation of the POPG headgroups, with increasing concentrations of SP-B_{59-80} are less than half those seen for KL_4. Changes caused by SP-B_{59-80} can be attributed to the peptide generally affecting lipid-lipid interactions rather than a direct electrostatic

interaction with the POPG headgroups. However, addition of either peptide leads to increases in the time averaged deuterium order parameters for the DPPC lipids, particularly at carbons 9-15. These increases suggest equally deep penetration of the peptides into the DPPC:POPG bilayers and are similar in scale for both peptides. For both peptides a transmembrane orientation is unlikely as this would place 3-4 polar amino acids into the bilayer interior. In this regard, our observations support KL_4 and SP-B_{59-80} partitioning similarly into DPPC:POPG lipid bilayers.

In 3:1 POPC-d_{31}:POPG lipids, the changes in the ^{31}P CSAs for the lamellar vesicles on addition of SP-B_{59-80} are smaller than those seen in 4:1 DPPC:POPG samples or on addition of KL_4 to POPC:POPG mixtures. However, at 2.5 mol% SP-B_{59-80}, a striking difference is seen in the ^{31}P powder patterns suggesting the onset of exchange between the lipid lamellar phase and a more dynamic lipid phase. The ^2H NMR order parameters decrease with increasing peptide concentrations. These increases in fatty acid mobility are similar to the trends found for KL_4, but the changes with SP-B_{59-80} are considerably greater in magnitude. These findings indicate that the SP-B_{59-80} remains in the interfacial region of the lipid bilayers at lower concentrations. At 2.5 mol% SP-B_{59-80}, a large coalesced peak in the center of the ^2H spectrum appears indicating the formation of a second, non-bilayer lipid phase is occurring. The ^{31}P and ^2H NMR data are consistent with the formation of small vesicles with motions that are fast on the NMR timescale, and may also implicate SP-B_{59-80} in lipid shuttling, lysis or degradation. Lipid lysis and degradation has been suggested as one of the many functions of SP-B that could be necessary for effective surfactant recycling and remediation [58,59]. An antimicrobial function has also been attributed to SP-B, and the lipid dynamics seen at 2.5 mol% SP-B_{59-80} are similar to behavior seen with higher concentrations of amphipathic antimicrobial peptides such as LL37, pardaxin, magainin, and synthetic derivatives [27,45,46,60]. This function is of particular interest as well to the saposin protein family, of which SP-B is the most hydrophobic member; this family includes several proteins which bind and traffic lipids for enzymatic modification or degradation [5]. However, further studies are needed to differentiate between either a role for SP-B_{59-80} in lipid degradation or in forming nonlamellar phases. Interestingly, we only saw this effect in 3:1 POPC:POPG, and not in DPPC:POPG at 2.5 mol% SP-B_{59-80}. This suggests the activity of SP-B_{59-80} is dependent on the saturation level of the acyl chains in a concentration dependent manner and provides a means of discrimination between lipids in the dynamic lung environment.

Based on the CD, ^{31}P NMR and ^2H NMR data, a model of how SP-B_{59-80} interacts with these lipid systems can be put forth (Figure 12). It should be noted that in this model we assume that SP-B_{59-80} is helical in a lipid environment, based on our CD data, and we propose that the peptide assumes an orientation in which the helix axis is perpendicular to the membrane normal due to the occurrence of charged residues throughout the primary sequence. Such an assumption is valid given the findings in the literature pertaining to the helical nature of SP-B and in particular the C-terminal region [8, 13, 61, 62]. However, from examination of the primary amino acid sequence and our ^2H NMR derived order parameters it is conceivable that the type of helical structure SP-B_{59-80} adopts may not be a canonical α-helix and the pitch of the helix may change as the peptide more deeply penetrates into the saturated lipid environments. For KL_4, this type of structural transition has been observed by solid state MAS NMR experiments (Mills, F.D. and Long, J.R., unpublished data). To answer the question of the type of helix SP-B_{59-80} forms in a lipid environment, similar MAS NMR experiments on ^{13}C labeled peptide in complex with lipids need to be performed.

Since an increase in DPPC acyl chain ordering is seen on addition of SP-B_{59-80} to 4:1 DPPC:POPG lipid vesicles, we conclude the peptide penetrates deeply into the hydrophobic region of the lipids and restricts acyl chain motion. In 3:1 POPC:POPG lipid vesicles, the disordering of the acyl chains indicate that the peptide is at the lipid/buffer interface in this

lipid system. This is consistent with the CD data which shows solely a helical conformation for SP-B_{59-80} when it is interacting with 4:1 DPPC:POPG vesicles, suggesting complete binding of the peptide, and a mixture of helix and random coil when it is interacting with 3:1 POPC:POPG vesicles, suggesting the peptide might partition between the lipid interface and aqueous phases. The results for addition of SP-B_{59-80} to DPPC:POPG suggest the peptide may deeply penetrate into the bilayer with the charged sidechains "snorkeling" to the interface as we have previously postulated to occur for KL_4. The snorkeling hypothesis is particularly relevant to KL_4 since all of the charged residues are lysines. However, while SP-B_{59-80} also has periodically spaced charged residues the aspartic acid sidechains are not as long and would not interact as favorably with the phosphate moieties. We are currently pursuing EPR and NMR studies which will allow refinement of our model. This will yield more accurate information in terms of orientation, depth penetration and structure of the peptide at particular amino acids. However, from the current study we can conclude that SP-B_{59-80} interactions with lung surfactant lipids and subsequent changes in lipid dynamics are dependent on the level of fatty acid saturation. While SP-B_{59-80} and KL_4 behave similarly in this regard, key differences are also evident. In particular, SP-B_{59-80} is able to alter bilayer structure in POPC:POPG vesicles at a concentration as low as 2.5 mol% while KL_4 is able to facilitate phase separation in DPPC:POPG vesicles. The phase separation characteristics of KL_4 may be of key relevance to the peptide's success in the clinic and can most likely be attributed to the use of solely positively charged residues rather than a mixture of cationic and anionic residues. The properties of SP-B_{59-80} in POPC:POPG vesicles may be due to the fact that polar and charged residues are spaced every four residues instead of every five residues leading to subtle changes in the structure and interaction of the peptide with the lipid lamellae relative to KL_4; alternatively electrostatic interactions may lead to the peptide being even more peripherally located in the lipid/water interface in comparison to KL_4.

Acknowledgements

We thank Profs. Art Edison, Gail Fanucci, and Manish Mehta for helpful discussions. The assistance of Dr. Alfred Chung in peptide synthesis and of the Molecular Structure Facility at University of California, Davis in AAA analysis is gratefully acknowledged. The research herein was funded by NIH 1R01HL076586 awarded to JRL. Support from the NSF National High Magnetic Field Laboratory and University of Florida is also gratefully acknowledged. ES wishes to acknowledge the financial support of the Natural Sciences and Engineering Research Council of Canada (NSERC).

References

1. Whitsett JA, Nogee LM, Weaver TE, Horowitz AD. Human Surfactant Protein-B - Structure, Function, Regulation, and Genetic-Disease. Physiol Rev 1995;75:749–757. [PubMed: 7480161]
2. Sarin VK, Gupta S, Leung TK, Taylor VE, Ohning BL, Whitsett JA, Fox JL. Biophysical and Biological-Activity of a Synthetic 8.7-Kda Hydrophobic Pulmonary Surfactant Protein Sp-B. P Natl Acad Sci USA 1990;87:2633–2637.
3. Revak SD, Merritt TA, Hallman M, Heldt G, Lapolla RJ, Hoey K, Houghten RA, Cochrane CG. The Use of Synthetic Peptides in the Formation of Biophysically and Biologically-Active Pulmonary Surfactants. Pediatric Research 1991;29:460–465. [PubMed: 1896249]
4. Johansson J, Curstedt T. Molecular structures and interactions of pulmonary surfactant components. Eur J Biochem 1997;244:675–93. [PubMed: 9108235]
5. Munford RS, Sheppard PO, O'Hara PJ. Saposin-like proteins (SAPLIP) carry out diverse functions on a common backbone structure. J Lipid Res 1995;36:1653–63. [PubMed: 7595087]
6. Mingarro I, Lukovic D, Vilar M, Perez-Gil J. Synthetic pulmonary surfactant preparations: New developments and future trends. Curr Med Chem 2008;15:393–403. [PubMed: 18288994]
7. Seurynck SL, Patch JA, Barron AE. Simple, helical peptoid analogs of lung surfactant protein B. Chem Biol 2005;12:77–88. [PubMed: 15664517]

8. Cochrane CG, Revak SD. Pulmonary surfactant protein B (SP-B): structure-function relationships. Science 1991;254:566–8. [PubMed: 1948032]
9. Waring A, Taeusch W, Bruni R, Amirkhanian J, Fan B, Stevens R, Young J. Synthetic amphipathic sequences of surfactant protein-B mimic several physicochemical and in vivo properties of native pulmonary surfactant proteins. Pept Res 1989;2:308–13. [PubMed: 2562485]
10. Waring AJ, Walther FJ, Gordon LM, Hernandez-Juviel JM, Hong T, Sherman MA, Alonso C, Alig T, Braun A, Bacon D, Zasadzinski JA. The role of charged amphipathic helices in the structure and function of surfactant protein B. Journal of Peptide Research 2005;66:364–374. [PubMed: 16316452]
11. Bruni R, Taeusch HW, Waring AJ. Surfactant Protein-B - Lipid Interactions of Synthetic Peptides Representing the Amino-Terminal Amphipathic Domain. P Natl Acad Sci USA 1991;88:7451–7455.
12. Kang JH, Lee MK, Kim KL, Hahm KS. The relationships between biophysical activity and the secondary structure of synthetic peptides from the pulmonary surfactant protein SP-B. Biochem Mol Biol Int 1996;40:617–627. [PubMed: 8908373]
13. Booth V, Waring AJ, Walther FJ, Keough KMW. NMR structures of the C-terminal segment of surfactant protein B in detergent micelles and hexafluoro-2-propanol. Biochemistry 2004;43:15187–15194. [PubMed: 15568810]
14. Sarker M, Waring AJ, Walther FJ, Keough KMW, Booth V. Structure of mini-B, a functional fragment of surfactant protein B, in detergent micelles. Biochemistry 2007;46:11047–11056. [PubMed: 17845058]
15. Cochrane CG, Revak SD, Merritt A, Heldt GP, Hallman M, Cunningham MD, Easa D, Pramanik A, Edwards DK, Alberts MS. The efficacy and safety of KL(4)-surfactant in infants with respiratory distress syndrome. Am J Resp Crit Care 1996;153:404–410.
16. Cochrane CG, Revak SD, Merritt TA, Schraufstatter IU, Hoch RC, Henderson C, Andersson S, Takamori H, Oades ZG. Bronchoalveolar lavage with KL4-Surfactant in models of meconium aspiration syndrome. Pediatric Research 1998;44:705–715. [PubMed: 9803452]
17. Wiswell TE, Smith RM, Katz LB, Mastroianni L, Wong DY, Willms D, Heard S, Wilson M, Hite RD, Anzueto A, Revak SD, Cochrane CG. Bronchopulmonary segmental lavage with surfaxin (KL4-surfactant) for acute respiratory distress syndrome. Am J Resp Crit Care 1999;160:1188–1195.
18. Sinha SK, Lacaze-Masmonteil T, Soler AVI, Wiswell TE, Gadzinowski J, Hajdu J, Bernstein G, d'Agostino R, STAR Dist. A multicenter, randomized, controlled trial of lucinactant versus poractant alfa among very premature infants at high risk for respiratory distress syndrome. Pediatrics 2005;115:1030–1038. [PubMed: 15805381]
19. Ghodrat M. Lung surfactants. Am J Health Syst Pharm 2006;63:1504–21. [PubMed: 16896079]
20. Vandenbussche G, Clercx A, Clercx M, Curstedt T, Johansson J, Jornvall H, Ruysschaert JM. Secondary Structure and Orientation of the Surfactant Protein Sp-B in a Lipid Environment - a Fourier-Transform Infrared-Spectroscopy Study. Biochemistry 1992;31:9169–9176. [PubMed: 1390703]
21. Wustneck N, Wustneck R, Perez-Gil J, Pison U. Effects of oligomerization and secondary structure on the surface behavior of pulmonary surfactant proteins SP-B and SP-C. Biophys J 2003;84:1940–9. [PubMed: 12609896]
22. Gustafsson M, Vandenbussche G, Curstedt T, Ruysschaert JM, Johansson J. The 21-residue surfactant peptide (LysLeu4)4Lys(KL4) is a transmembrane alpha-helix with a mixed nonpolar/polar surface. FEBS Lett 1996;384:185–8. [PubMed: 8612820]
23. Cai P, Flach CR, Mendelsohn R. An infrared reflection-absorption spectroscopy study of the secondary structure in (KL4)4K, a therapeutic agent for respiratory distress syndrome, in aqueous monolayers with phospholipids. Biochemistry 2003;42:9446–52. [PubMed: 12899632]
24. Antharam VC, Elliott DW, Mills FD, Farver RS, Sternin E, Long JR. The penetration depth of surfactant peptide KL4 into membranes is determined by fatty acid saturation. 2008submitted
25. Mills FD, Antharam VC, Elliott DW, McNeill SA, Long JR. The helical structure of surfactant peptide KL4 when bound to POPC: POPG lipid vesicles. Biochemistry. 2008In Press
26. Terzi E, Holzemann G, Seelig J. Interaction of Alzheimer beta-amyloid peptide(1-40) with lipid membranes. Biochemistry 1997;36:14845–52. [PubMed: 9398206]

27. Ramamoorthy A, Thennarasu S, Lee DK, Tan A, Maloy L. Solid-state NMR investigation of the membrane-disrupting mechanism of antimicrobial peptides MSI-78 and MSI-594 derived from magainin 2 and melittin. Biophys J 2006;91:206–16. [PubMed: 16603496]
28. Wieprecht T, Apostolov O, Beyermann M, Seelig J. Thermodynamics of the alpha-helix-coil transition of amphipathic peptides in a membrane environment: implications for the peptide-membrane binding equilibrium. J Mol Biol 1999;294:785–94. [PubMed: 10610796]
29. Veldhuizen R, Nag K, Orgeig S, Possmayer F. The role of lipids in pulmonary surfactant. Bba-Mol Basis Dis 1998;1408:90–108.
30. Kuliopulos A, Walsh CT. Production, Purification, and Cleavage of Tandem Repeats of Recombinant Peptides. J Am Chem Soc 1994;116:4599–4607.
31. Chen PS, Toribara TY, Warner H. Microdetermination of Phosphorus. Anal Chem 1956;28:1756–1758.
32. Sternin E, Schafer H, Polozov IV, Gawrisch K. Simultaneous determination of orientational and order parameter distributions from NMR spectra of partially oriented model membranes. J Magn Reson 2001;149:110–3. [PubMed: 11273758]
33. Petrache HI, Dodd SW, Brown MF. Area per lipid and acyl length distributions in fluid phosphatidylcholines determined by (2)H NMR spectroscopy. Biophys J 2000;79:3172–92. [PubMed: 11106622]
34. Seelig A, Seelig J. The dynamic structure of fatty acyl chains in a phospholipid bilayer measured by deuterium magnetic resonance. Biochemistry 1974;13:4839–45. [PubMed: 4371820]
35. Chapman R, Kulp JL, Patgiri A, Kallenbach NR, Bracken C, Arora PS. Trapping a folding intermediate of the alpha-helix: Stabilization of the pi-helix. Biochemistry 2008;47:4189–4195. [PubMed: 18335996]
36. Andrade MA, Chacon P, Merelo JJ, Moran F. Evaluation of Secondary Structure of Proteins from Uv Circular-Dichroism Spectra Using an Unsupervised Learning Neural-Network. Protein Engineering 1993;6:383–390. [PubMed: 8332596]
37. Saenz A, Canadas O, Bagatolli LA, Johnson ME, Casals C. Physical properties and surface activity of surfactant-like membranes containing the cationic and hydrophobic peptide KL4. Febs J 2006;273:2515–27. [PubMed: 16704424]
38. Ma JW, Koppenol S, Yu HU, Zografi G. Effects of a cationic and hydrophobic peptide, KL4, on model lung surfactant lipid monolayers. Biophysical Journal 1998;74:1899–1907. [PubMed: 9545051]
39. Qiu X, Mirau PA, Pidgeon C. Magnetically induced orientation of phosphatidylcholine membranes. Biochim Biophys Acta 1993;1147:59–72. [PubMed: 8466932]
40. Seelig J, Borle F, Cross TA. Magnetic-Ordering of Phospholipid-Membranes. Biochimica Et Biophysica Acta 1985;814:195–198.
41. Seelig J. 31P nuclear magnetic resonance and the head group structure of phospholipids in membranes. Biochim Biophys Acta 1978;515:105–40. [PubMed: 356883]
42. Bunow MR, Levin IW. Raman-Spectra and Vibrational Assignments for Deuterated Membrane Lipids - 1,2-Dipalmitoyl Phosphatidylcholine-D9 and 1,2-Dipalmitoyl Phosphatidylcholine-D62. Biochimica Et Biophysica Acta 1977;489:191–206. [PubMed: 579158]
43. Seelig J, Seelig A. Lipid conformation in model membranes and biological membranes. Q Rev Biophys 1980;13:19–61. [PubMed: 7220788]
44. Burnett LJ, Muller BH. Deuteron Quadrupole Coupling Constants in 3 Solid Deuterated Paraffin Hydrocarbons-C2d6, C4d10, C6d14. J Chem Phys 1971;55:5829–&.
45. Henzler-Wildman KA, Martinez GV, Brown MF, Ramamoorthy A. Perturbation of the hydrophobic core of lipid bilayers by the human antimicrobial peptide LL-37. Biochemistry 2004;43:8459–8469. [PubMed: 15222757]
46. Porcelli F, Buck B, Lee DK, Hallock KJ, Ramamoorthy A, Veglia G. Structure and orientation of pardaxin determined by NMR experiments in model membranes. Journal of Biological Chemistry 2004;279:45815–45823. [PubMed: 15292173]
47. Abu-Baker S, Qi XY, Lorigan GA. Investigating the interaction of saposin c with POPS and POPC phospholipids: A solid-state NMR spectroscopic study. Biophysical Journal 2007;93:3480–3490. [PubMed: 17704143]

48. Abu-Baker S, Qi XY, Newstadt J, Lorigan GA. Structural changes in a binary mixed phospholipid bilayer of DOPG and DOPS upon saposin C interaction at acidic pH utilizing P-31 and H-2 solid-state NMR spectroscopy. Bba-Biomembranes 2005;1717:58–66. [PubMed: 16289479]

49. Huster D, Dietrich U, Gutberlet T, Gawrisch K, Arnold K. Lipid matrix properties in cationic membranes interacting with anionic polyelectrolytes: A solid-state NMR approach. Langmuir 2000;16:9225–9232.

50. Laroche G, Dufourc EJ, Pezolet M, Dufourcq J. Coupled Changes between Lipid Order and Polypeptide Conformation at the Membrane-Surface - a H-2 Nmr and Raman-Study of Polylysine Phosphatidic-Acid Systems. Biochemistry 1990;29:6460–6465. [PubMed: 2207087]

51. Stockton GW, Smith ICP. Deuterium Nuclear Magnetic-Resonance Study of Condensing Effect of Cholesterol on Egg Phosphatidylcholine Bilayer Membranes. 1. Perdeuterated Fatty-Acid Probes. Chem Phys Lipids 1976;17:251–263. [PubMed: 1033045]

52. Oldfield E, Meadows M, Rice D, Jacobs R. Spectroscopic Studies of Specifically Deuterium Labeled Membrane Systems - Nuclear Magnetic-Resonance Investigation of Effects of Cholesterol in Model Systems. Biochemistry 1978;17:2727–2740. [PubMed: 687560]

53. Nezil FA, Bloom M. Combined Influence of Cholesterol and Synthetic Amphiphillic Peptides Upon Bilayer Thickness in Model Membranes. Biophysical Journal 1992;61:1176–1183. [PubMed: 1600079]

54. de Planque MR, Greathouse DV, Koeppe RE 2nd, Schafer H, Marsh D, Killian JA. Influence of lipid/peptide hydrophobic mismatch on the thickness of diacylphosphatidylcholine bilayers. A 2H NMR and ESR study using designed transmembrane alpha-helical peptides and gramicidin A. Biochemistry 1998;37:9333–45. [PubMed: 9649314]

55. Vogt B, Ducarme P, Schinzel S, Brasseur R, Bechinger B. The topology of lysine-containing amphipathic peptides in bilayers by circular dichroism, solid-state NMR, and molecular modeling. Biophysical Journal 2000;79:2644–2656. [PubMed: 11053137]

56. Perkins WR, Dause RB, Parente RA, Minchey SR, Neuman KC, Gruner SM, Taraschi TF, Janoff AS. Role of lipid polymorphism in pulmonary surfactant. Science 1996;273:330–2. [PubMed: 8662513]

57. Moya FR, Gadzinowski J, Bancalari E, Salinas V, Kopelman B, Bancalari A, Kornacka MK, Merritt TA, Segal R, Schaber CJ, Tsai H, Massaro J, d'Agostino R. A multicenter, randomized, masked, comparison trial of lucinactant, colfosceril palmitate, and beractant for the prevention of respiratory distress syndrome among very preterm infants. Pediatrics 2005;115:1018–29. [PubMed: 15805380]

58. Ryan MA, Akinbi HT, Serrano AG, Perez-Gil J, Wu HX, McCormack FX, Weaver TE. Antimicrobial activity of native and synthetic surfactant protein B peptides. J Immunol 2006;176:416–425. [PubMed: 16365435]

59. Weaver TE, Conkright JJ. Function of surfactant proteins B and C. Annu Rev Physiol 2001;63:555–78. [PubMed: 11181967]

60. Bechinger B. Detergent-like properties of magainin antibiotic peptides: a 31P solid-state NMR spectroscopy study. Biochim Biophys Acta 2005;1712:101–8. [PubMed: 15869740]

61. Ye Q, Biltonen RL. Differential scanning and dynamic calorimetric studies of cooperative phase transitions in phospholipid bilayer membranes. Subcell Biochem 1994;23:121–60. [PubMed: 7855872]

62. Cochrane CG, Revak SD. Protein-phospholipid interactions in pulmonary surfactant. The Parker B. Francis Lectureship. Chest 1994;105:57S–62S. [PubMed: 8131614]

Abbreviations used

SP-B
surfactant protein B

NMR
nuclear magnetic resonance

CD
circular dichroism

DSC
differential scanning calorimetry

MLV
multilamellar vesicle

LUV
large unilamellar vesicle

L_α
fluid lamellar phase

L_β
gel lamellar phase

POPC
1-palmitoyl-2-oleoyl-*sn*-glycero-3-phosphatidylcholine

POPC-d_{31}
1-d_{31}-palmitoyl-2-oleoyl-*sn*-glycero-3-phosphatidylcholine

POPG
1-palmitoyl-2-oleoyl-*sn*-glycero-3-phosphatidylglycerol

DPPC
1,2-dipalmitoyl-*sn*-Glycero-3-Phosphocholine

DPPC-d_{62}
1,2-d_{62}-dipalmitoyl-*sn*-Glycero-3-Phosphocholine

P/L
peptide/lipid molar ratio

H_{II}
inverted hexagonal phase

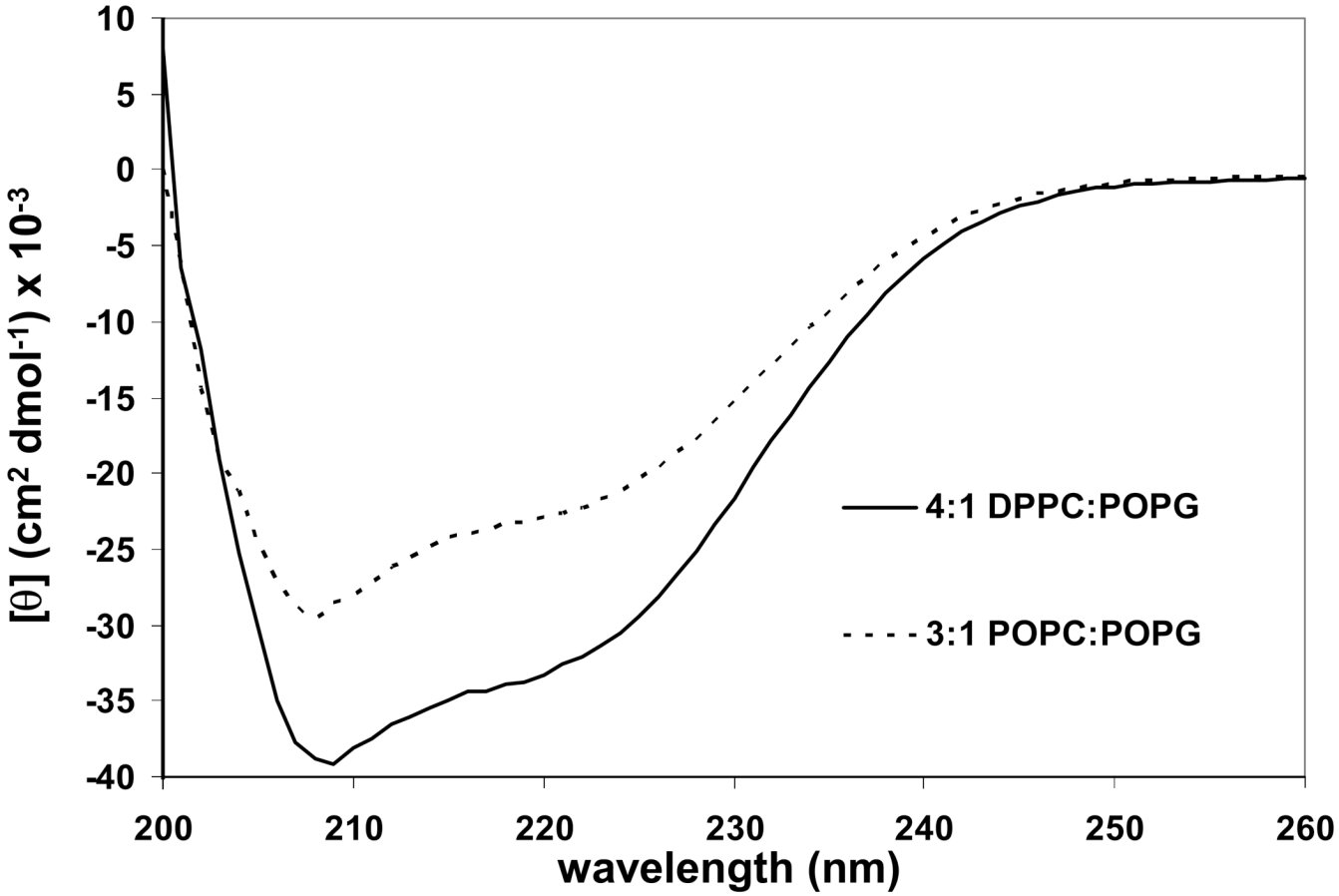

Figure 1.
CD spectra at 45 °C of SP-B′$_{59-80}$ at a P:L molar ratio of 1:100 in 4:1 DPPC:POPG (------) and 3:1 POPC:POPG (- - - - - -). The final peptide concentration was 40 μM.

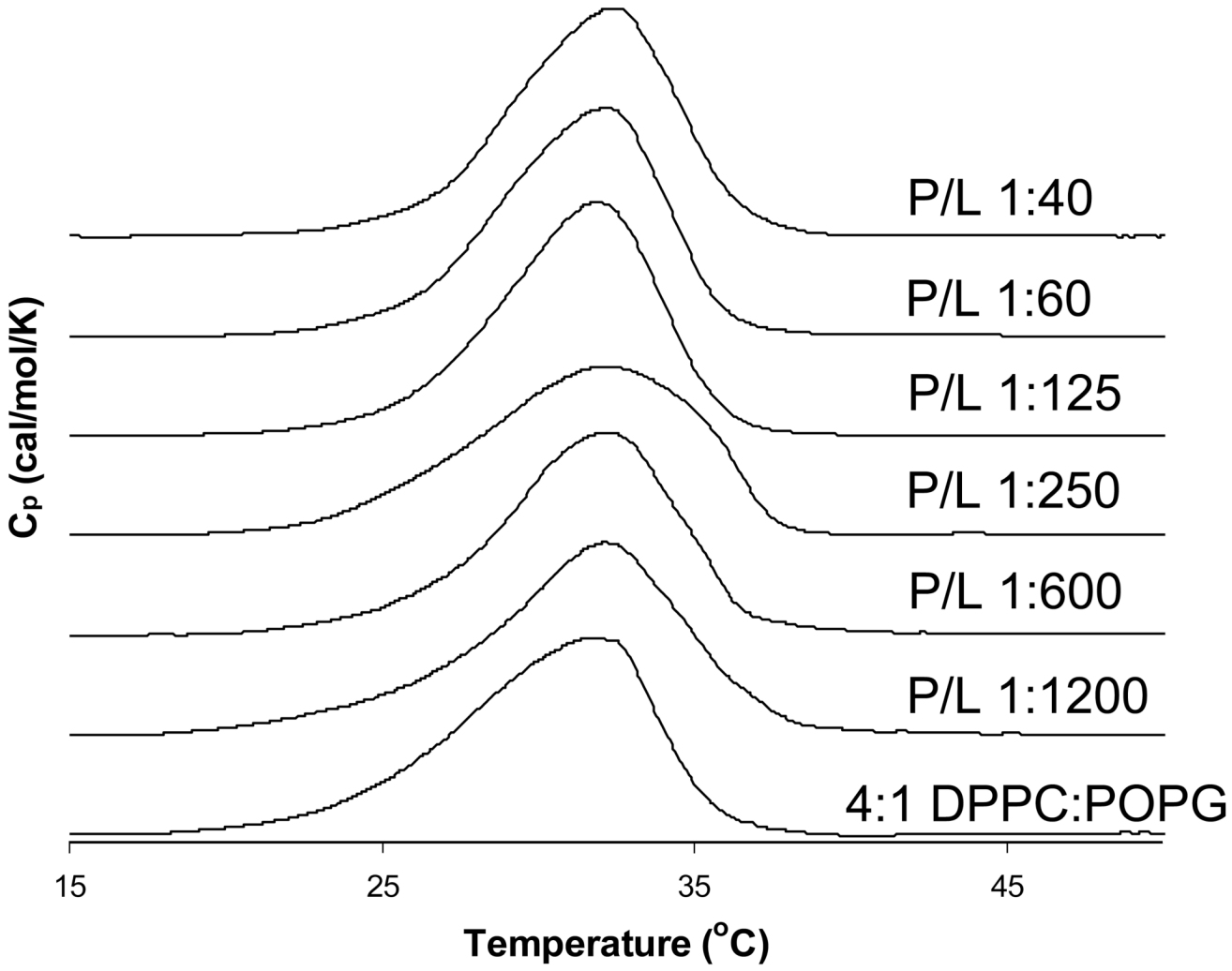

Figure 2.
DSC scans for 4:1 DPPC-d_{62}:POPG LUVs with SP-$B_{59\text{-}80}$ at the indicated P:L molar ratios.

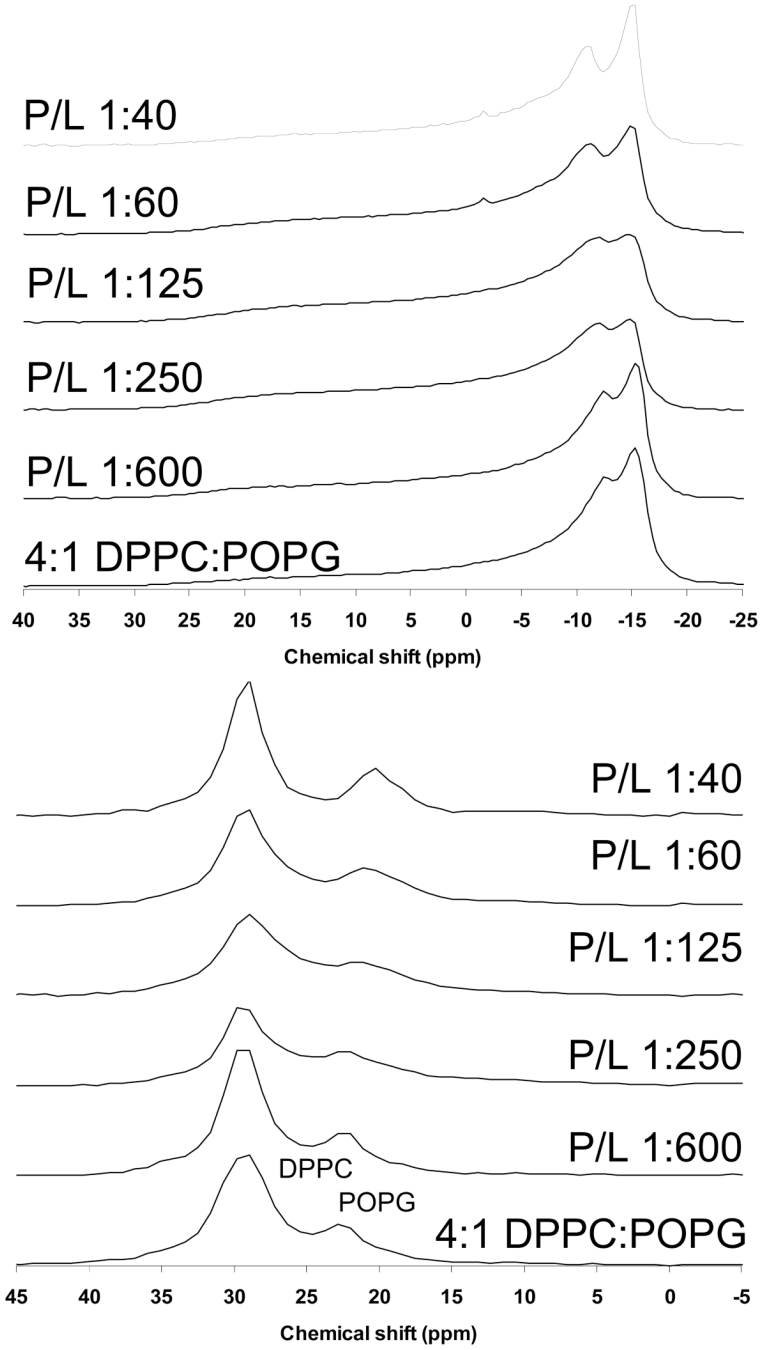

Figure 3.
Phosphorous NMR spectra of 4:1 DPPC-d_{62}:POPG MLVs with SP-$B_{59\text{-}80}$ at the indicated P:L molar ratios. (Top) Static NMR spectra and (Bottom) DePaked spectra. Spectra were collected at 44 °C.

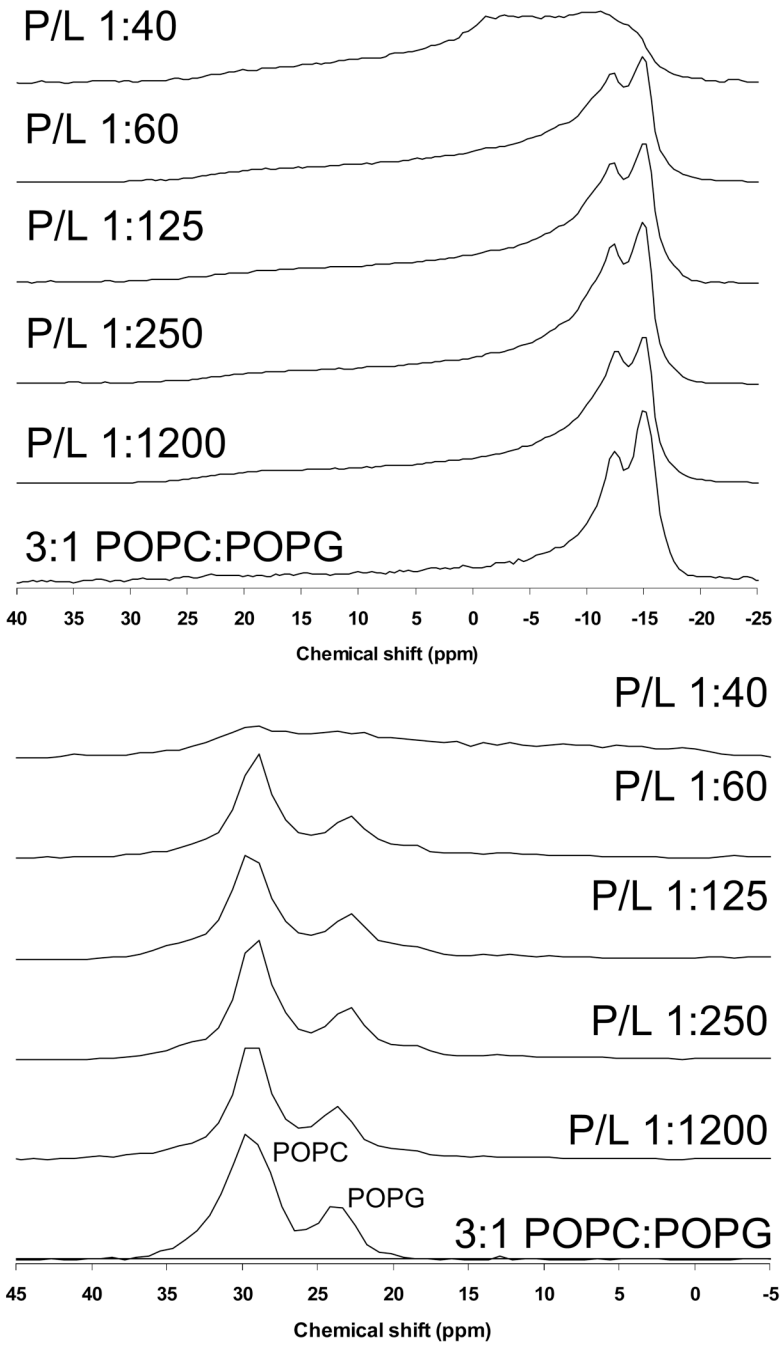

Figure 4.
Phosphorous NMR spectra of 3:1 POPC-d_{31}:POPG MLVs with SP-$B_{59\text{-}80}$ at the indicated P:L molar ratios. (Top) Static NMR spectra and (Bottom) DePaked spectra. Spectra were collected at 44 °C.

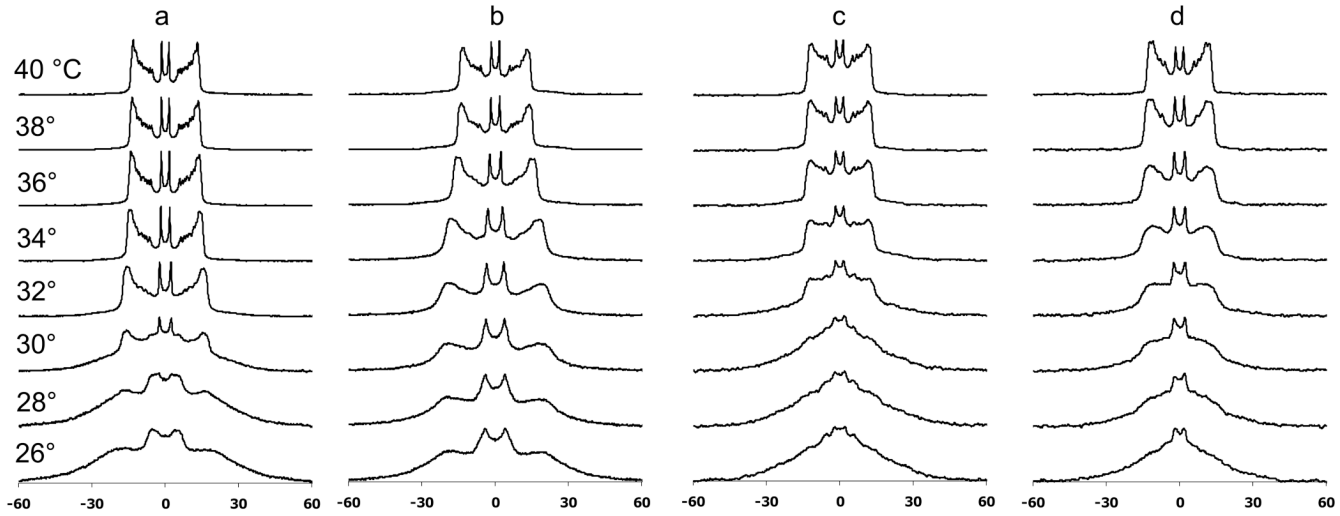

Figure 5.

Deuterium NMR spectra as a function of temperature for a) 4:1 DPPC-d_{62}:POPG MLVs, b) 4:1 DPPC-d_{62}:POPG MLVs with SP-B′$_{59-80}$ at a P:L molar ratio of 1:100, c) 4:1 DPPC:POPG-d_{31} MLVs, and d) c) 4:1 DPPC:POPG-d_{31} MLVs with SP-B′$_{59-80}$ at a P:L molar ratio of 1:100.

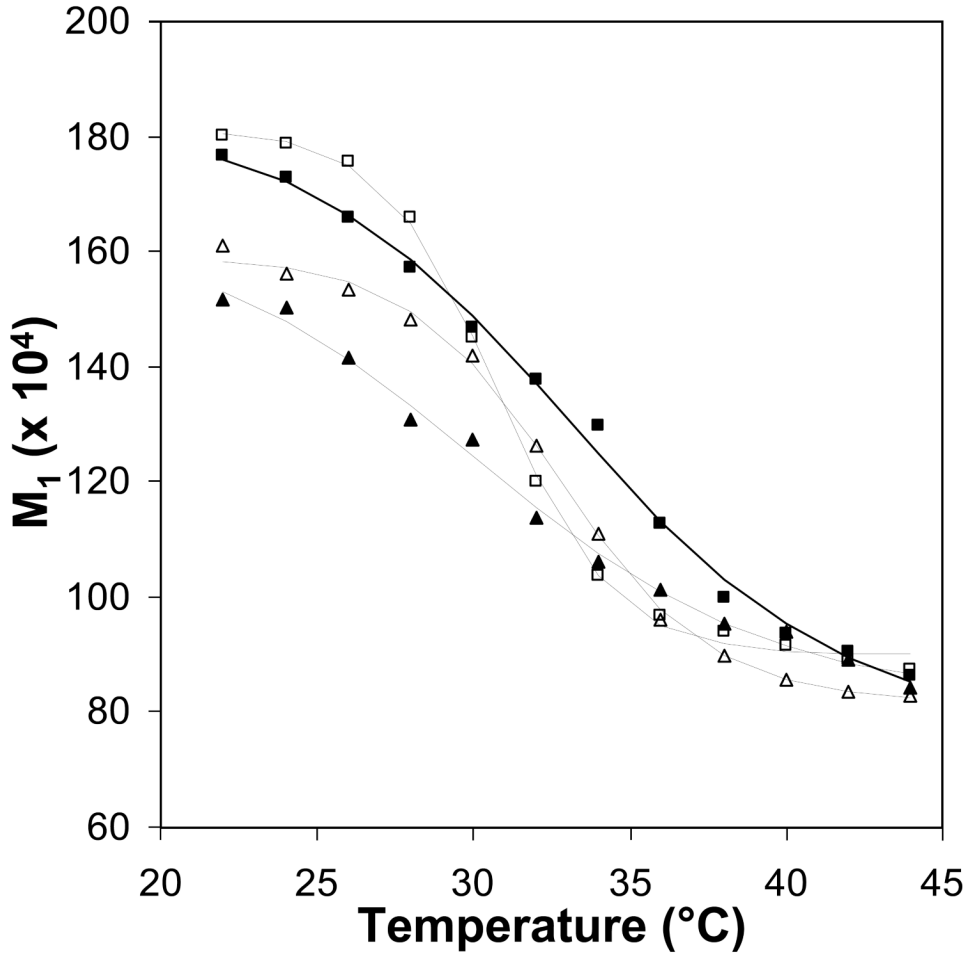

Figure 6.

First moment, M_1, as a function of temperature for the ^{2}H NMR spectra plotted in Figure 5; data for 4:1 DPPC-d_{62}:POPG MLVs (open squares), 4:1 DPPC-d_{62}:POPG MLVs with SP-B $'_{59\text{-}80}$ at a P:L molar ratio of 1:100 (closed squares), 4:1 DPPC:POPG-d_{31} MLVs (open triangles), and 4:1 DPPC:POPG-d_{31} MLVs with SP-B$'_{59\text{-}80}$ at a P:L molar ratio of 1:100 (closed triangles) show the variations in the melting temperatures of the lipids on addition of peptide.

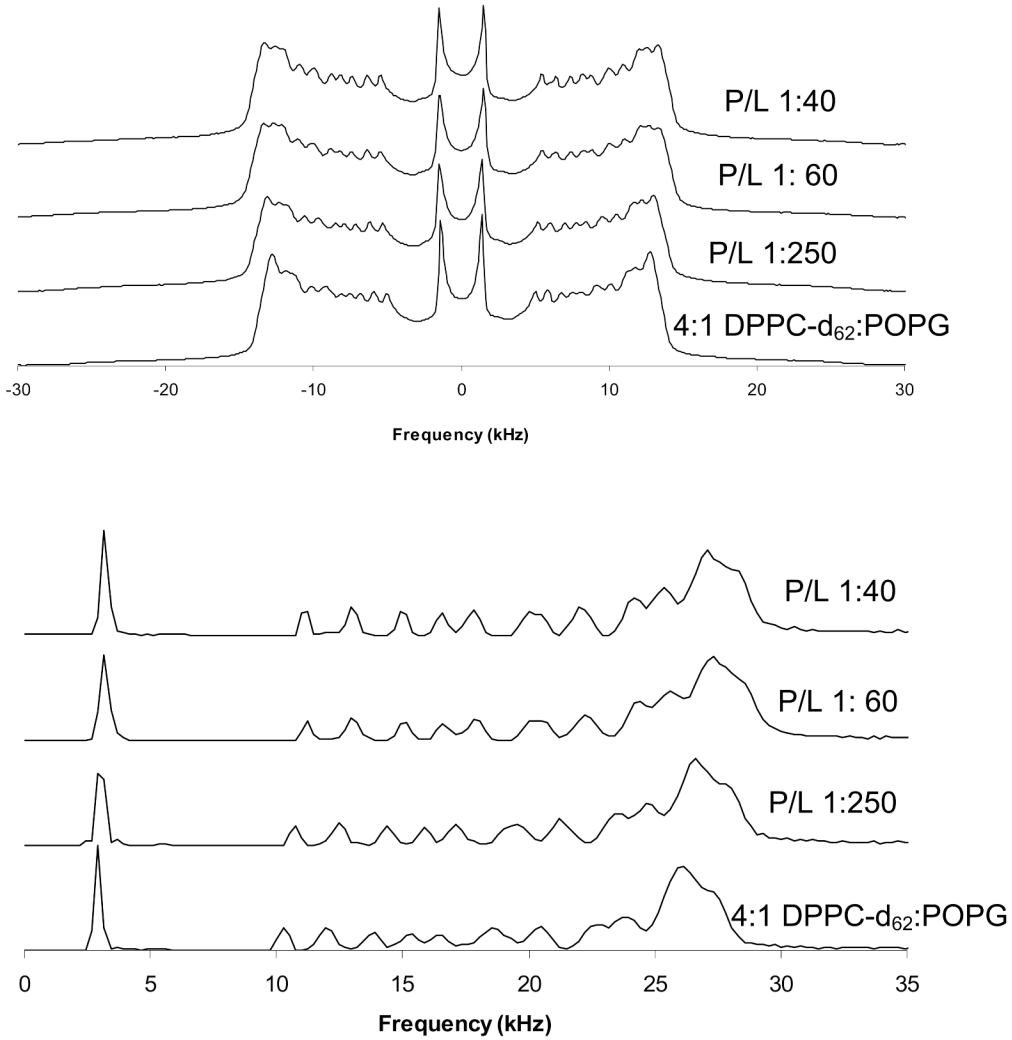

Figure 7.

Deuterium NMR spectra of 4:1 DPPC-d_{62}:POPG MLVs with SP-B_{59-80} at the indicated P:L molar ratios. Spectra were taken at 44 °C. (Top) Static NMR spectra; (Bottom) dePaked spectra.

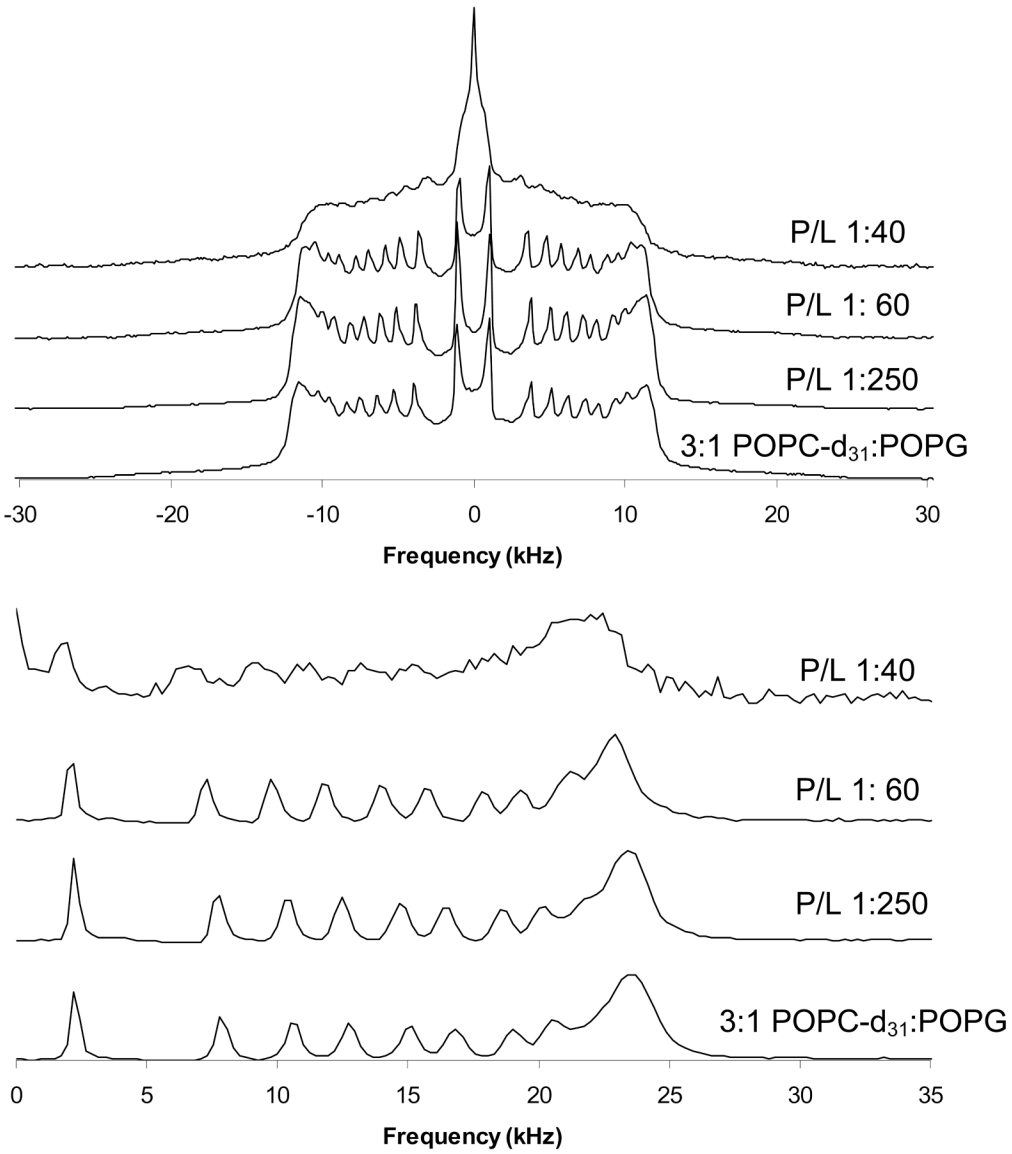

Figure 8.

Deuterium NMR spectra of 3:1 POPC-d_{31}:POPG MLVs with SP-$B_{59\text{-}80}$ at the indicated P:L molar ratios. Spectra were taken at 44 °C. (Top) Static NMR spectra and (Bottom) dePaked spectra.

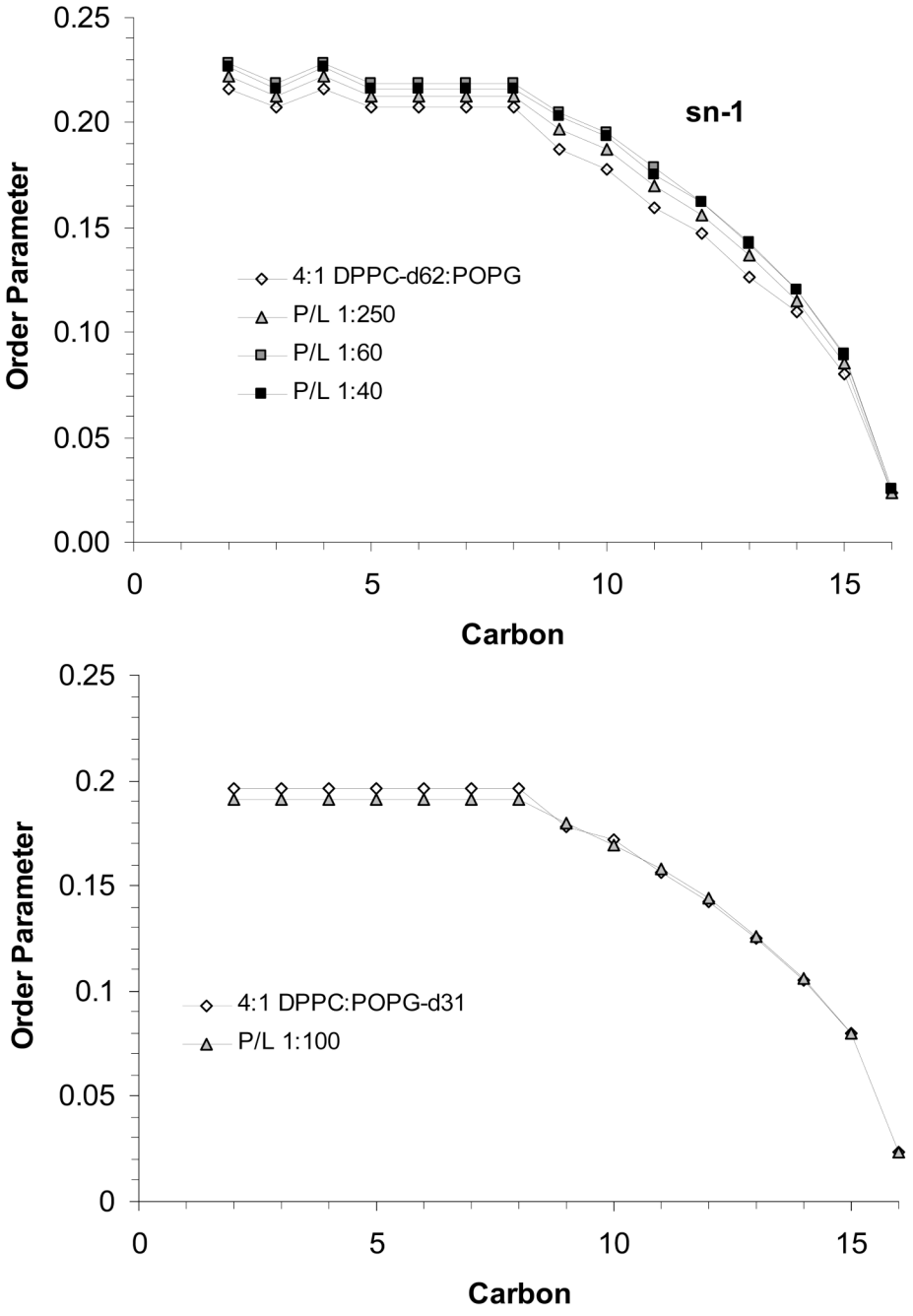

Figure 9.
Order parameter profiles for the *sn*-1 chains of DPPC-d_{62} (top) and POPG-d_{31} (bottom) in 4:1 DPPC:POPG MLVs at 44 °C with SP-B_{59-80} at the indicated P:L molar ratios.

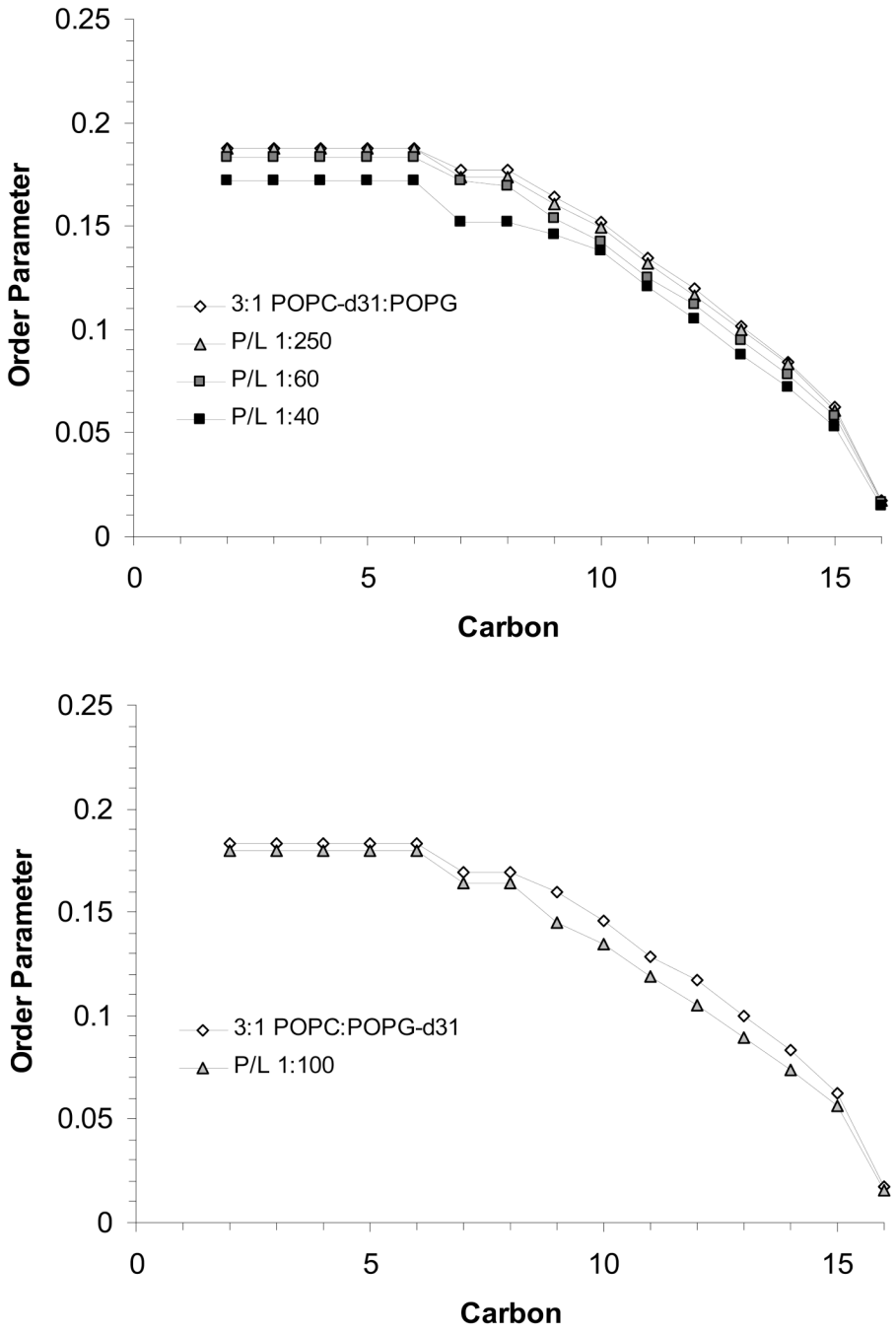

Figure 10.
Order parameter profiles for the *sn*-1 chains of POPC-d_{31} (top) and POPG-d_{31} (bottom) in 3:1 POPC:POPG MLVs at 44 °C with SP-$B_{59\text{-}80}$ at the indicated P:L molar ratios.

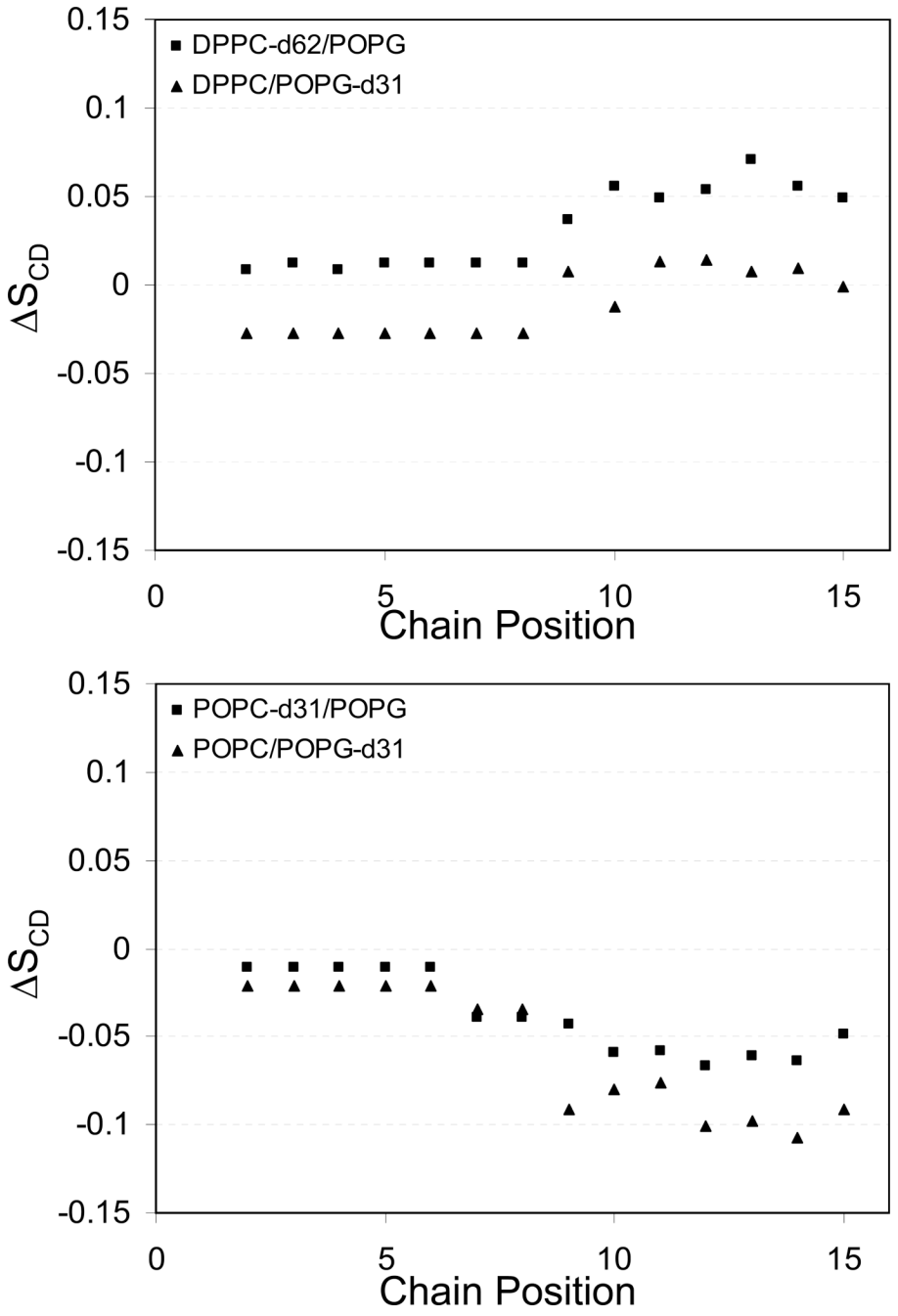

Figure 11.
Changes in d_{31}-palmitoyl acid chain order parameters in 4:1 DPPC:POPG MLVs (top) and 3:1 POPC:POPG MLVs (bottom) on addition of SP-B′$_{59\text{-}80}$ at a P:L molar ratio of 1:100.

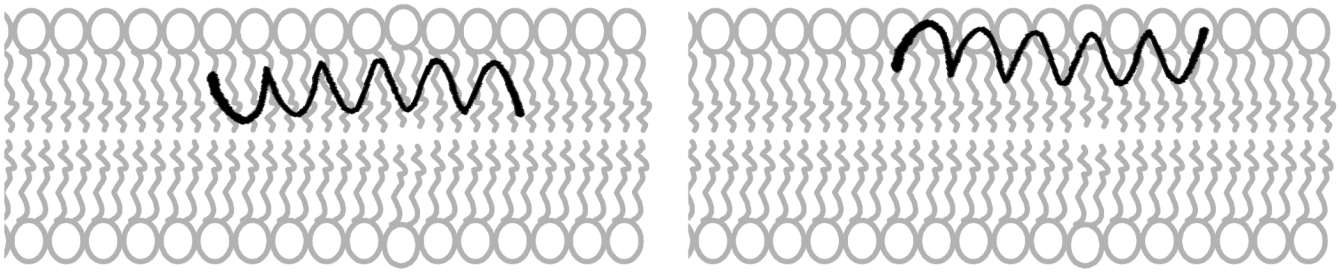

Figure 12.
Models of SP-B_{59-80} interactions with the two lipid environments studied assuming a helical peptide conformation. (Left) Based on ^2H NMR data, SP-B_{59-80} deeply penetrates into 4:1 DPPC:POPG lipid bilayers. (Right) In contrast, in 3:1 POPC:POPG MLVs lipids, a more peripheral interaction of SP-B_{59-80} with the lipid headgroup region is proposed. A transmembrane orientation of the peptide is unlikely as it would place four polar residues in the hydrophobic interior.